Estimates of future flow, including extremes, of the Columbia River headwaters

Gerd Bürger, J. Schulla, & Arelia T. Werner

2011

Pacific Climate Impacts Consortium (PCIC)

PCIC Publications

Original citation:

Bürger, G., Schulla, J., & Werner, A. T. (2011). Estimates of future flow, including extremes, of the Columbia River headwaters. *Water Resources Research*, *47*(10), W10520. https://doi.org/10.1029/2010WR009716

Estimates of future flow, including extremes, of the Columbia River headwaters

G. Bürger,[1] J. Schulla,[1] and A. T. Werner[1]

Received 2 July 2010; revised 6 September 2011; accepted 7 September 2011; published 20 October 2011.

[1] Streamflow projections, including extremes, for the 2050s for the Columbia River headwaters above Donald are obtained by downscaling four regional climate models of the North American Regional Climate Change Assessment Program (NARCCAP) suite and subsequent driving of a hydrologic model. We employ the entire model chain from global and regional climate models, station-based statistical downscaling, and a fully distributed, physically based hydrologic model and verify the results against observed streamflow. The performance is model dependent but is generally encouraging enough to justify the application of the climate scenarios. A general warming of about 2°C is projected and, on average, slightly drier conditions, especially in late summer. We find evidence that the projected changes are elevation dependent and relatively small scale, with decreasing signals with higher elevations. All models project a shift of the hydrograph toward a more rain-fed regime, with peak flows occurring in June instead of July. Annual peak flow is projected to not increase, and August low flow decreases in all four models. With nonshrinking (static) glaciers, relatively high melting rates are simulated for August and September that partly compensate for the shifted hydrograph; this enhanced glacier melt is also detected in simulated historic Columbia headwater flow. The static approximation is supported by a heuristic seasonal sensitivity analysis that suggests a moderate average areal glacier recession of about 10% for the midcentury. We discuss the need for a dynamic glacier component for a refined assessment of future drought risk.

Citation: Bürger, G., J. Schulla, and A. T. Werner (2011), Estimates of future flow, including extremes, of the Columbia River headwaters, *Water Resour. Res., 47*, W10520, doi:10.1029/2010WR009716.

1. Introduction

[2] In a warmer world, precipitation increasingly falls as rain instead of snow. For mountainous watersheds, the time-delaying effect of snow will therefore be reduced, and hydrographs become more rainfall dominated, with stronger spring and early summer runoff and reduced water supply in late summer and fall [*Barnett et al.*, 2005; *Stewart et al.*, 2005; *Knowles et al.*, 2006]. Current observations, in fact, indicate that in some areas these changes are already underway [*Barnett et al.*, 2008; *Déry et al.*, 2009]. Moreover, with rising temperatures it becomes increasingly likely that all the snow of the previous season is melted, and excess heat is able to melt the accumulated ice volume of past years, leading to a slow retreat of glaciers. But since warmer air holds more moisture and since more water evaporates over the oceans, precipitation tends to become more intense. The exact nature of this precipitation response is, however, very complicated and strongly depends on season, latitude, coastal proximity, topography, and natural fluctuations, all of which are only imperfectly represented in current global climate models (GCMs). Mountainous terrain, moreover, with its processes of snow accumulation and melting, creates a memory in the local climate and a coupling of temperature and precipitation whose balance is very delicate. All this affects river flow as an accumulated climate response through the seasons over variable terrain. Its simulation and future projection from climate models requires multiple temporal and spatial scales to be represented with considerable accuracy, a task that is quite challenging and loaded with uncertainty.

[3] The Pacific Northwest, in particular the Columbia River basin, is one example where understanding streamflow response to a changing climate is difficult and uncertain and, at the same time, the possible impact on the water supply and society is potentially dramatic. The Columbia River is a significant resource to residents of the United States and Canada. It is managed for water supply, used to generate hydropower, and contained to prevent flooding. The Columbia River Treaty (1964) regulates the water resources between the United States and Canada (http://www.empr.gov.bc.ca/EAED/EPB/Pages/CRT.aspx). These regulations, which bind both parties until 2024, do not take climate change into account but will very likely do so should the treaty be continued.

[4] There exists a fairly large body of literature on the climatic impact on the Columbia River, both for some tributaries and for the whole basin. Much of this impact is due to natural fluctuations and the proximity to the Pacific Ocean [*Cayan*, 1996; *McCabe and Dettinger*, 2002; *McCabe et al.*, 2004]. *Leung et al.* [1999] study the impact

[1]Pacific Climate Impacts Consortium, Victoria, British Columbia, Canada.

0043-1397/11/2010WR009716

of the El Niño–Southern Oscillation (ENSO), along with the Pacific Decadal Oscillation (PDO), on the hydrology of the Columbia basin; *Hamlet et al.* [2005] and *Mote et al.* [2005] interpret historic hydrologic trends in the Pacific Northwest; *Payne et al.* [2004] study "business-as-usual" climate scenarios and their impact on the Columbia from a water resource management point of view; and *Elsner et al.* [2009] review and update the present knowledge about the area by analyzing an entire range of up-to-date climate projections. In maritime climates, snow cover and hence summer streamflow are dominated by winter precipitation variability, which complicates the understanding of recent trends [*Hamlet et al.*, 2005; *Mote et al.*, 2005; *Stahl and Moore*, 2006]. Historic data of snowpack and glacier coverage show a consistent retreat, nevertheless [*Luckman and Kavanagh*, 2000; *Schiefer et al.*, 2007; *Bolch et al.*, 2010]. This is a global phenomenon [*Lemke et al.*, 2007], and it is widely believed to happen in response to a warming climate, with melting levels (in terms of ice volume) reaching 40% and more by the 2050s as compared to present conditions [*Oerlemans et al.*, 1998; *Schneeberger et al.*, 2003; *Meehl et al.*, 2007].

[5] Fewer studies have focused on smaller spatial scales by investigating subbasins of the Columbia [*Loukas et al.*, 2004; *Salathe*, 2005; *Vano et al.*, 2010a, 2010b]. For those, glacier coverage (with corresponding summer melting) increasingly contributes to the discharge and water levels downstream, so that glacier response to climate is quite relevant for such basins for the late summer months [*Stahl and Moore*, 2006; *Nolin et al.*, 2010].

[6] Common to the above studies is the projected shift in the mean behavior of the system, resulting in a shifted hydrologic regime from nival to pluvial. From a "user" perspective, assessments of the climatic impact on extremes, such as droughts and floods, are at least of comparable relevance but are only just emerging and, for obvious reasons, are loaded with uncertainty. For the Columbia basin, one study projects increasing flood likelihood by the end of the century for the southeastern part of the Columbia basin and little or no change elsewhere [cf. *Hamlet*, 2010]; in a related study, droughts are projected to become more severe for the southwestern part of the basin, with the other parts showing no change or even slight increases as in the Upper Columbia [see *Hamlet et al.*, 2010].

[7] Information about future climate variability ultimately comes from the daily variations of the simulated large-scale GCM fields. As daily GCM data are not a priori better or worse than monthly data, the main reason that they have not found a more widespread use in impact assessments is a practical one: limited public availability and obstacles in the data processing because of the size of the data. None of the above studies utilize daily GCM fields, however, as future daily variability is inferred from present daily historic series and future monthly data. Their usefulness for assessing future extremes is therefore limited to cases where a change in extremes is reflected in monthly statistics. The value added by using daily GCM data has been demonstrated by *Maurer et al.* [2010], who show that the simulation of high-flow and, particularly, low-flow statistics is improved for watersheds in California, United States.

[8] Likewise, projecting future high- and low-flow statistics is incomplete without refining the spatial resolution of the driving climate fields. And just as the potential of a shift in daily variability must be taken into account, a shift of the spatial pattern of climate change must also be taken into account. That means not only must the driving climate fields be provided with sufficient spatial detail, a procedure commonly referred to as "downscaling" [e.g., *Wilby and Wigley*, 1997] and virtually always employed by current climate impact studies, but also must the downscaling allow for spatially varying climate signals.

[9] The present study is the first of its kind to address the question of future low and high flow for the headwaters of the Columbia River by employing a two-step downscaling (dynamical followed by statistical) that provides both submonthly and subgrid-scale data flexible enough to allow for their possible changes in the future. Specifically, for both the present and future we use four of the dynamically downscaled GCM simulations of the North American Regional Climate Change Assessment Program (NARCCAP [*Mearns et al.*, 2005]). These will further be statistically downscaled to station scale using the expanded downscaling (EDS) method of *Bürger* [1996], whose output will finally be used to drive the fully distributed, physically based hydrologic model WaSim [*Schulla and Jasper*, 2000]. WaSim in its current version uses static glacier hydrology; the importance of future glacier runoff is heuristically assessed by estimating glacier change from seasonal sensitivity characteristics. For the hydrometric gauge at Donald, whose watershed is shown in Figure 1, we thus obtain an ensemble of present and future streamflow simulations.

[10] It must be stressed that the focus of this study is methodological, as several modeling elements are combined here for the first time. Accordingly, there is substantial need for validation, which we do by analyzing the entire model chain from the atmospheric analyses down to the measured daily streamflow at the Donald gauge. Because present and future flow is simulated from static glaciers the importance of glacier dynamics for extreme, especially late summer, low flow is discussed. To keep the study contained, we have focused solely on the projected seasonal hydrograph and extreme flow. A more in-depth hydrologic analysis of the scenarios, including the single effects on snow, rain, or groundwater, is not given.

2. The Study Area

[11] The Columbia watershed above Donald is situated in the Canadian Rocky Mountains between Donald and the Canal Flats, south of (and part of) Yoho National Park. It is fed by a number of glaciers from the Canadian Rockies, including the Wapta ice field with the Yoho glacier, and the Columbia Mountains. The size of the basin is 9716 km^2, with an altitudinal range from 769 to 3420 m. About 3%, or 288 km^2, is covered by glaciers. This part of the river is unregulated and therefore suitable for hydrologic modeling.

[12] Past annual records of areal temperature anomalies and, to represent glacier melt, August streamflow for the basin reveal a strong positive trend for the former ($+0.01°C = +2\%$ of detrended standard deviation per year) and a slightly negative trend for the latter ($-0.25\ m^3\ s^{-1} = -0.4\%$ of detrended standard deviation per year); see Figure 2. The trend is significantly nonzero for temperature (using the Mann-Kendall test with $\alpha = 0.05$). For streamflow the trend

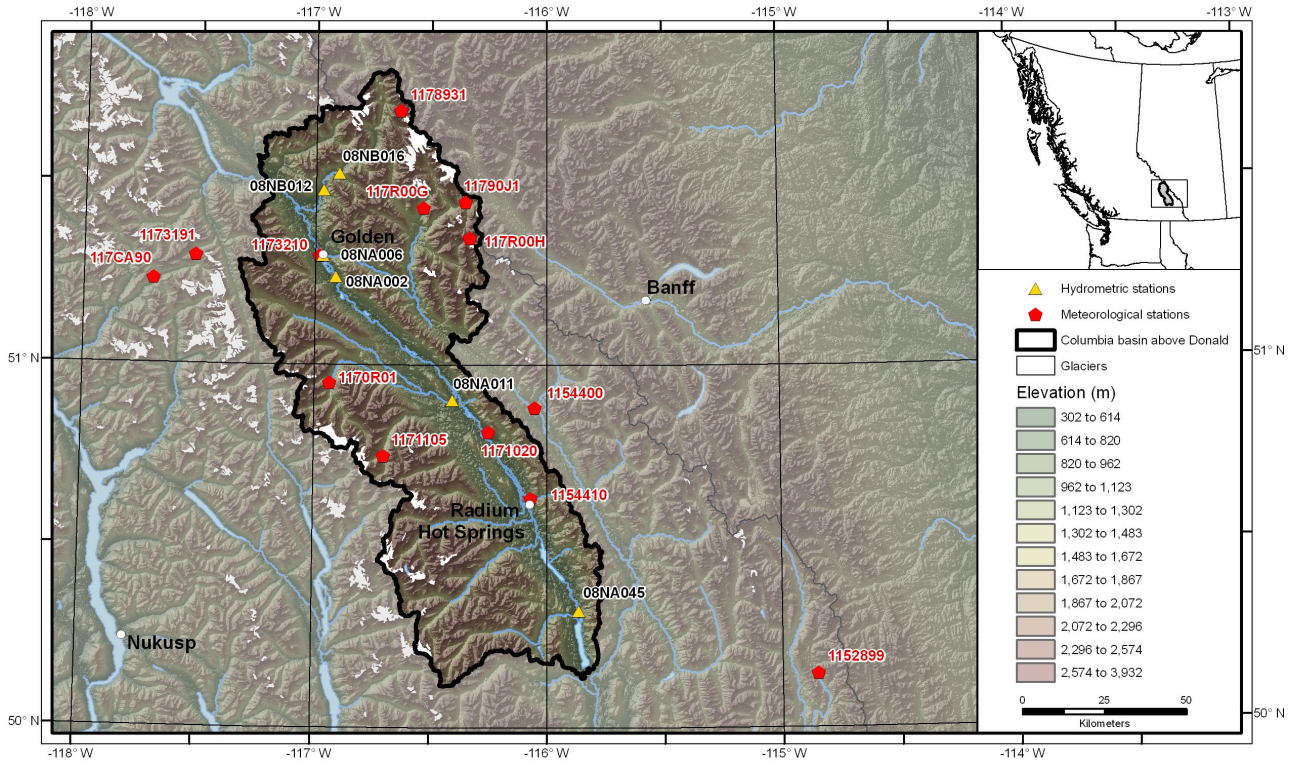

Figure 1. The study area of the Columbia River headwaters (above Donald).

is insignificant (even for a level of $\alpha = 0.1$), and it remains so even when accounting for interannual climate variations, as described by *Stahl and Moore* [2006]. It is therefore uncertain whether the basin is already negatively affected by the warming conditions, a tendency that has been reported for glaciated basins of British Columbia by *Stahl and Moore* [2006]. It is the purpose of this study to analyze the effect of climatic change on the Columbia headwaters, especially with respect to high and low flows, the latter of which includes the negative effects of retreating glaciers.

3. Methods and Data

[13] Our climate impact analysis will be conducted using several of the North American climate simulations available

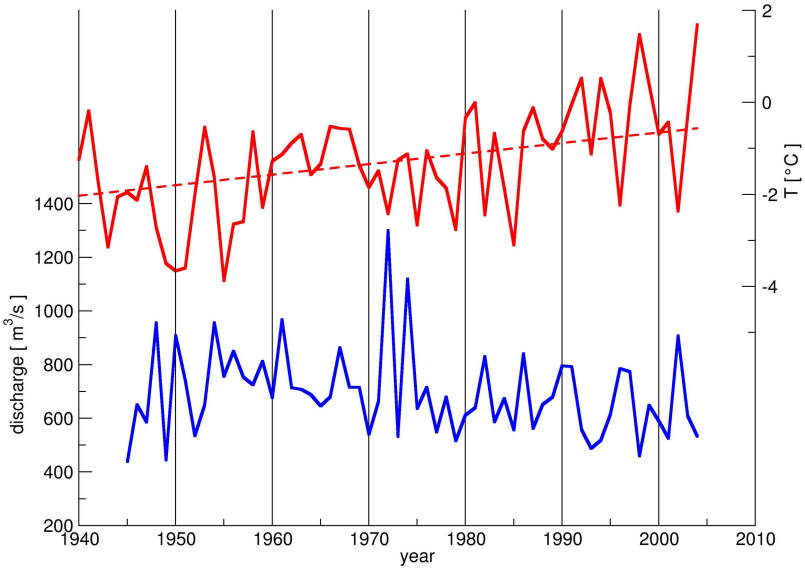

Figure 2. Annual areal temperature (red line) and Columbia discharge at Donald for August (blue line). Temperature is taken as a mean anomaly across all stations and shows a significant positive trend. Discharge has no significant trend.

from the NARCCAP project [*Mearns et al.*, 2005]. These are simulations from an array of regional climate models (RCMs) driven by (nested in) the large-scale global atmosphere, either analyzed or simulated by GCMs using external radiative forcings representing present (20C3M [*Meehl et al.*, 2005]) and future (A2 [*Intergovernmental Panel on Climate Change*, 2000]) conditions. The analyzed global atmosphere is given by the National Centers for Environmental Prediction (NCEP) Reanalysis II data for the period 1979–2004 [*Kanamitsu et al.*, 2002]. Only RCM/GCM combinations that had, at the time of writing, complete simulations for both present and future climate were considered. As displayed in Table 1 these are the NCEP-driven runs of CRCM [*Caya and Laprise*, 1999], HRM3 [*Hudson and Jones*, 2002], and RCM3 [*Pal et al.*, 2006], as well as present and future driving simulations of the three GCMs, CGCM3, HADCM3, and GFDL2.1. All RCMs are run at a spatial resolution of 50 km. NARCCAP does not contain transient climate simulations; these would have been necessary when employing a dynamic glacier model that evolves over time.

[14] Given the strong topographic gradients of the study area, it is important to provide climatic information at sufficiently fine areal scale. The added value of RCMs has been demonstrated for the Columbia River by *Leung et al.* [1999] and *Payne et al.* [2004], with the latter study finding that increased spatial detail helps to resolve positive temperature snow-albedo feedbacks. Representing regional precipitation is, nonetheless, considerably more challenging. For NARCCAP, *Wang et al.* [2009] report strong precipitation biases for areas comparable to the study area and advise caution in using the NARCCAP precipitation directly. Removing this bias and providing as much climatic detail as possible, including detail of change, are achieved by employing a station-based statistical downscaling that is able to respond to climate change by station and, subsequently, a 500 m interpolation that considers orographic effects on temperature and precipitation, as described, e.g., by *Alpert* [1986] and *Barros and Lettenmaier* [1994].

[15] Meteorological observations (MET) are minimum and maximum temperature, T_n and T_x, and precipitation P from the Canadian daily climate data set [*Environment Canada*, 2007], shown in Table 2; we will occasionally use $T = (T_n + T_x)/2$ as a proxy for daily average temperature. It must be noted that prior to 1990, there are large data gaps for many stations, especially those in the mountainous regions, which are bound to impact all statistical estimates, not least the downscaling model. Streamflow observations are from the Water Survey of Canada (http://www.ec.gc.ca/rhc-wsc/). We refer to the various coupled simulations simply as MET, 20C3M, A2, etc., to highlight the specific drivers.

[16] Figure 3 displays the flow of model information in our study. Starting with present and future atmospheric conditions, analyzed or simulated, the corresponding fields are statistically downscaled and, along with meteorological observations, are fed into a hydrologic model. If all planned NARCCAP simulations were available, this would give a total of $(2 \times 3 + 1) \times 3 + 1 = 22$ streamflow simulations. At the time of this writing, only seven were actually available, which were all NCEP-driven runs and CRCM driven by CGCM3, HRM3 driven by HADCM3, and RCM3 driven by GFDL and CGCM3 for both present (20C3M) and future climates (A2).

Table 1. Matrix of the NARCCAP General Circulation Model (GCM) Runs Driving Regional Climate Models (RCMs)

	NCEP	CGCM3	HADCM3	GFDL
CRCM	X	X		
HRM3	X		X	
RCM3	X	X		X

3.1. Expanded Downscaling

[17] Expanded downscaling is born out of the idea to simulate local meteorological events that are as close as possible to and consistent with the prevailing atmospheric circulation but at the same time generate local covariability (of variables and stations) that is realistic enough to be used for studying the climatic impact on extremes, such as floods and droughts, and to drive corresponding impact models.

[18] To formulate the problem, let us assume we have selected, for a record of local variables $\mathbf{y}(t)$, a set of atmospheric predictor fields $\mathbf{x}(t)$. One seeks a transfer function $f: \mathbf{x}(t) \mapsto \mathbf{y}(t)$ that maps $\mathbf{x}$ as close as possible to $\mathbf{y}$. Using least squares regression is usually a satisfactory solution if the prevailing correlations between $\mathbf{x}$ and $\mathbf{y}$ are sufficiently high. For low correlations, however, the regression approach is too "conservative" because it relies on climatology to avoid larger errors and thus loses much of the variability. One needs to find a compromise between the defining regression rules of absolute error minimization and the realistic variability and practical use of stochastic weather generators. This can be formulated mathematically as a constraint optimization problem, which leads to a unique, albeit approximate, solution that is quite expensive to estimate [*Bürger*, 1996]. However, by relating the EDS problem to similar problems from statistical shape analysis [*Dryden and Mardia*, 1998], it is possible to recast EDS as an orthogonal Procrustes problem, which then leads to the following closed form solution:

$$\begin{aligned} \mathbf{U\Sigma V} &= \mathbf{G_y y' x G_x^{-1}}, \\ \mathrm{EDS} &= \mathbf{G_x^{-1} V U' G_y}, \end{aligned} \tag{1}$$

where the first equation is the singular value decomposition (SVD) and $\mathbf{G_x}$ and $\mathbf{G_y}$ denote the Cholesky factors of $\mathbf{x'x}$ and $\mathbf{y'y}$, respectively.

[19] EDS is a linear model that operates on large-scale, daily atmospheric field anomalies $\mathbf{x(t)}$ and simulates corresponding daily local "weather" $\mathbf{y(t)}$ [*Bürger*, 1996]; it is particularly suited and has been frequently applied to the climate downscaling of hydrologic extremes [*Müller-Wohlfeil et al.*, 2000; *Bürger*, 2002; *Menzel and Bürger*, 2002; *Bürger and Chen*, 2005; *Menzel et al.*, 2006] and has recently been extended to numerical weather forecasts [*Bürger*, 2009; *Bürger et al.*, 2009]. It may be worth noting that like any other station-based downscaling employing a transfer function, EDS enables each single station and variable to respond individually to climate change. This is unlike, e.g., so-called delta approaches where a given historic data set is adjusted or scaled to match a given climate

Table 2. Climate and Hydrometric Stations, With Altitudes and Areas

ID	Name[a]	Latitude	Longitude	Altitude (m)	Area (km^2)	Type
1152899	Fording River Cominco	50.15	−114.85	1585		climate
1154400	Kootenay NP Kootenay Crossing	50.88	−116.05	1170		climate
1154410	Kootenay NP West Gate	50.63	−116.07	899		climate
1170R01	Bobbie Burns	50.95	−116.93	1370		climate
1173191	Glacier NP Rogers Pass	51.30	−117.52	1323		climate
1173210	Golden A	51.30	−116.98	785		climate
117CA90	Glacier NP Mount Fidelity	51.23	−117.70	1875		climate
117R00G	Yoho NP Emerald Lake	51.43	−116.54	1303		climate
117R00H	Yoho NP Ohara Lake	51.35	−116.33	2027		climate
1171020	Brisco	50.82	−116.26	823		climate
1171105	Bugaboo Creek Lodge	50.75	−116.70	1494		climate
1178931	Wildcat Creek Mistaya Lodge	51.70	−116.64	2057		climate
11790J1	Yoho Park	51.44	−116.34	1615		climate
08NB005	Columbia River at Donald	51.48	−117.18	9710		hydrometric
08NA002	Columbia at Nicholson	51.24	−116.91		6660	hydrometric
08NA045	Fairmont Hot Springs	50.32	−115.86		891	hydrometric
08NA006	Kicking Horse	51.30	−116.97		1850	hydrometric
08NA011	Spillimacheen	50.90	−116.40		1430	hydrometric
08NB016	Split Creek	51.53	−116.90		81	hydrometric
08NB012	Blaeberry River	51.48	−116.97		588	hydrometric

[a]NP, National Park.

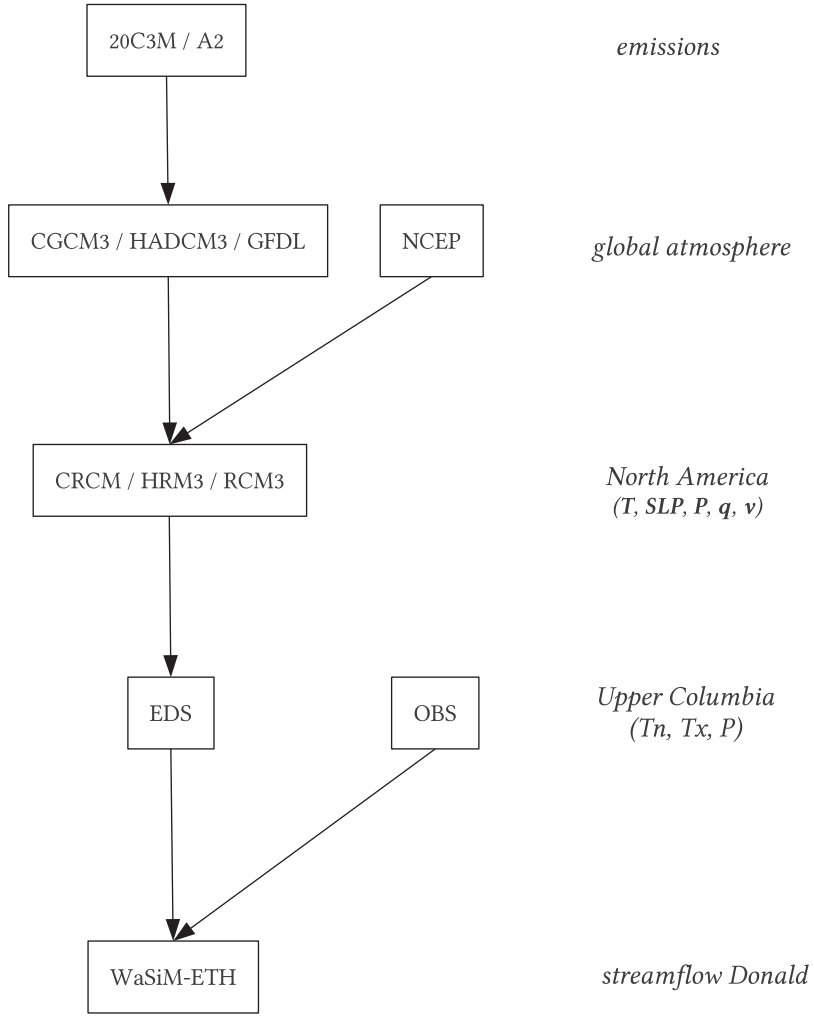

Figure 3. Overview of model flow.

anomaly (using a "delta"; this is sometimes called a spatial or temporal delta method, depending on the primary type of adjustment) that is uniform over a larger domain [e.g., *Hamlet and Lettenmaier*, 1999; *Loukas et al.*, 2004; *Payne et al.*, 2004; *Elsner et al.*, 2009]. The corresponding consequences are discussed in section 5.

[20] For this study, we have used the following daily surface fields from the area between the bounding corner points (124°W, 46°N) and (110°W, 53°N): specific humidity **q**, precipitation **P**, sea level pressure (**SLP**), air temperature **T**, and wind vector **v** (see Figure 3); all fields were projected onto the dominant set of empirical orthogonal functions of the NCEP-driven runs, so that 99% of the multivariate variability of the fields is represented by the corresponding principal components. Local station data are minimum and maximum temperature and precipitation, using the stations in Table 2. The calibration period was 1980–1997. Before calibration, all quantities (global and local) were normalized to a Gaussian distribution using the so-called "probit" [*Bürger*, 1996]. The probit parameters are part of the calibration, and in EDS applications they are used for rescaling the simulated Gaussian variables back to physical units. In particular, the probit parameters define the base annual cycle, so that any simulated climate change is treated as an anomaly from this base state.

[21] No climate model will ever reproduce the present or future climates with perfection because of incompleteness in sampling data and in the numeric representation of the physics. While the sampling problem can partly be overcome by using sufficiently long estimation periods [*Hawkins and Sutton*, 2009], the latter problem is inherent in the numeric approach and can never fully be recovered. Therefore, it has become standard practice to apply bias correction schemes when using simulated climates for driving impact models. While correcting for the mean is part of this standard, correcting for variability is less common, albeit equally important, and is done, for example, in quantile mapping schemes [e.g., *Wood et al.*, 2002; *Maurer et al.*, 2010]. Univariate correction schemes lead, however, to a general distortion of the multivariate covariance structure whose patterns are represented by the set of empirical orthogonal functions. As a consequence, for example, the main storm tracks can be biased. In cases where the full synoptic variability of a GCM is utilized (as in ours) one should apply multivariate bias correction. This technique is a direct mathematical analog of the univariate case, with (univariate) variance being replaced by (multivariate) covariance or, equivalently, standard deviation by Cholesky factors. Specifically, the multivariate simulated anomalies are multiplied by the matrix product of the inverse Cholesky factor of the simulated anomalies and the Cholesky factor of the observed anomalies. The details, which to our knowledge have not been described elsewhere, are given in Appendix A.

3.2. The Hydrologic Water Balance Simulation Model

[22] The Water Balance Simulation Model (WaSim [*Schulla*, 1997; *Schulla and Jasper*, 2007]) is a physically based, distributed hydrologic model. It has been applied to over 60 basins covering a wide range of climates, from arid to humid and from cold to hot (including Africa, Australia, South America, Asia, Europe, and the Arctic). The model can be run with a wide range of spatial and temporal resolutions from the centimeter to kilometer and seconds to days ranges. The following components were applied in this implementation of the model: (1) inverse distance weighting of meteorological input, combined with elevation-dependent regression, (2) potential evapotranspiration with approaches after *Hamon* [1963], (3) snow accumulation and melt approaches via degree-days, (4) glacier model accounting for ice, firn, and snow separately, (5) interception model (bucket approach with variable capacities), (6) multihorizon soil model using the Richards approach for unsaturated flow, (7) single-aquifer groundwater model, including base flow generation by exfiltration of groundwater into river channels, (8) lake modeling (inflow/outflow/volume rules), and (9) river routing with a kinematic wave approach including artificial inputs and abstractions.

[23] In the current study, WaSim was run at a spatial resolution of 500 m on a daily time step. The model was calibrated over the period from 1990 to 1997, using the same stations as EDS, listed in Table 2. The following spatial input data were used: (1) Digital Elevation Model based on the Shuttle Radar Topographic Mission, version 4 (~3 min resolution resampled to 100 m regularly spaced (i.e., Cartesian) grid; http://srtm.csi.cgiar.org/), (2) land use data based on the Advanced Very High Resolution Radiometer data distributed by Natural Resources Canada (http://geogratis.cgdi.gc.ca), (3) soil classification based on the physical data obtained from the Soils Program from *Global Soil Data Task Group* [2000], and (4) glacier boundaries from the GeoBC Service Desk (http://archive.ilmb.gov.bc.ca/crgb/products/mapdata/corporate_watershed_base_products.htm).

[24] The calibration was carried out manually. Fifteen runs were performed to set the basic parameters for the subbasins of the Columbia River above Fairmount Hot Springs, the Spillimacheen River, and the Kicking Horse River. Another 45 semiautomated runs were then used to optimize the parameters. During this process the need to include the lakes in the routing model became obvious. Two major lakes and a series of single linear reservoirs were applied to the routing schemes to consider the effects of meandering rivers in the flat valleys. As indicated, the simulation results are quite sensitive to the spatial distribution of the meteorological drivers, T and P, and therefore depend on the type of interpolation used. For both variables a simple nearest-neighbor technique was combined with a lapse rate approach. While one fixed lapse rate was sufficient for T, using an extra, flatter lapse rate for higher elevations (>2000 m) turned out to be crucial for P, in accordance with results of *Alpert* [1986; see also *Barros and Lettenmaier*, 1994]. The calibration, shown in Figure 4, resulted in a Nash-Sutcliffe efficiency (NSE) of 94.4% for the gauge at Donald, with a total difference in runoff volume of about 5.5%; for validation, the numbers are NSE = 95.0% and −3.5%, respectively. The average NSE of all subbasins was 86%. It is evident that the complex topography of the watershed is imperfectly represented by the 13 climate stations (see Figure 1), which can only be partially reconciled by applying interpolation. Large data gaps found in the data, especially in the 1980s, add to this problem.

3.3. Glaciers

[25] Glacier retreat, in terms of glacier dynamics, means that more ice is ablated below the "equilibrium line altitude" than is formed above that line, so that this line is

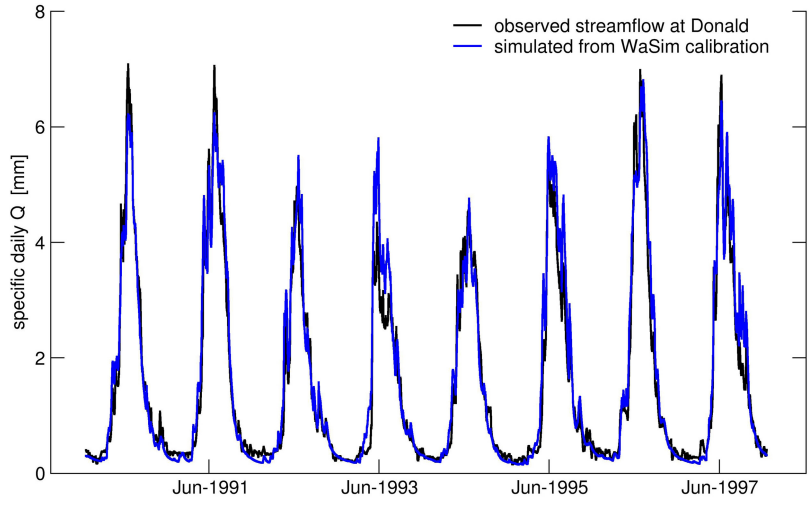

Figure 4. Calibration run of WaSim. The daily Nash-Sutcliffe efficiency is 94.4%.

rising. This process depends, however, on the delicate interplay between temperature and precipitation and is quite sensitive to spatial and temporal details. Surplus ice formation from increased winter precipitation, as projected by most GCMs, may very well counter the enhanced melting from higher summer temperatures. It is estimated that on (global) average, a precipitation increase of about 35% per 1 K warming is needed to counter glacier ablation [*Braithwaite et al.*, 2002]. This number is probably lower for the glaciers in the study area, which are at a relatively high elevation (see Figure 5), with precipitation falling as snow and a large turnover rate. Under such circumstances, glacier response to a warmer climate is dominated by precipitation [*Bitz and Battisti*, 1999].

[26] Glacier melting and corresponding runoff are roughly proportional to the glaciated area. The accompanying ice dynamics are, nevertheless, complicated functions of volume, geometry, and the environment of the glacier. On the other hand, there exists the following fairly simple scaling relation between the area A and volume V of an ice sheet:

$$V = aA^{\gamma}, \tag{2}$$

with universal constants of $a = 28.5$ and $\gamma = 1.36$ obtained from empirical as well as theoretical studies [*Chen and Ohmura*, 1990; *Bahr et al.*, 1997]. The water equivalent of this volume V of ice, measured as the height b of a corresponding water column, is related to the area A by the ratio of the respective densities of ice and water, $\rho_I = 850$ kg m^{-3} and ρ_W, as follows:

$$b = \frac{V}{A} = \frac{a\rho_I}{\rho_W} A^{\gamma-1}. \tag{3a}$$

[27] The corresponding inverse relation is given by

$$A = \left(\frac{b\rho_W}{a\rho_I}\right)^{\frac{1}{\gamma-1}}. \tag{3b}$$

[28] Using equations (3a) and (3b), it is possible to approximate the areal extent of a glacier by its mass (and mass balances are easier to estimate).

[29] The transition from the present to the future extent of the glacier involves the dynamic response of the ice mass to the driving climate. Depending on the degree of sophistication, the modeling of glacier extent and hydrology is more or less expensive in terms of external field data input and computation time [*Flowers et al.*, 2005; *Schaefli et al.*, 2005; *Huss et al.*, 2007, 2008; *Stahl et al.*, 2008]. Because, in the current version of WaSim, glaciers are treated statically and because a dynamic response would require a transient climate simulation anyway (which is not part of the NARCCAP suite), glacier dynamics in this study are approximated using a fairly simple, heuristic approach. Given a time horizon of a few decades (up to the 2050s), the equilibrium response of glaciers to a changing climate can be approximated linearly via the seasonal sensitivity characteristic (SSC) [*Oerlemans and Reichert*, 2000]. According to the SSC, glacier mass balance is determined from a set of 2×12 parameters describing the seasonal sensitivities (linear dependencies), c^T and c^P, of the glacier mass balance to temperature and precipitation anomalies as follows:

$$\Delta b = \sum_{i=1,12} c_i^T (T_i - T_{\mathrm{ref}}) + c_i^P (P_i - P_{\mathrm{ref}})/P_{\mathrm{ref}}, \tag{4}$$

where the subscript ref indicates some reference state. Using monthly anomalies, this model compares astoundingly well with both observations and simulations by a full mass-energy balance model, giving correlations of 0.97 on an annual basis [*Oerlemans and Reichert*, 2000]. Figure 6 shows the monthly SSC coefficients of the Peyto glacier in the Canadian Rocky Mountains, which is in close proximity to the study area. Note that from these sensitivities it follows that a 1 K increase of T (-0.39 m annually) must be countered by only about a 10% increase of P (0.32 m annually) to leave the glacier in balance, as compared to $\sim$35% estimated globally (see above).

[30] Applying the SSC to the mean monthly T and P anomalies of the 2050s (which are generally smaller than single monthly or annual fluctuations) provides the missing link between present and future glacier extent:

$$A(\text{present}) \overset{(3a)}{\rightarrow} b(\text{present}) \overset{(4)}{\rightarrow} b(\text{future}) \overset{(3b)}{\rightarrow} A(\text{future}). \tag{5}$$

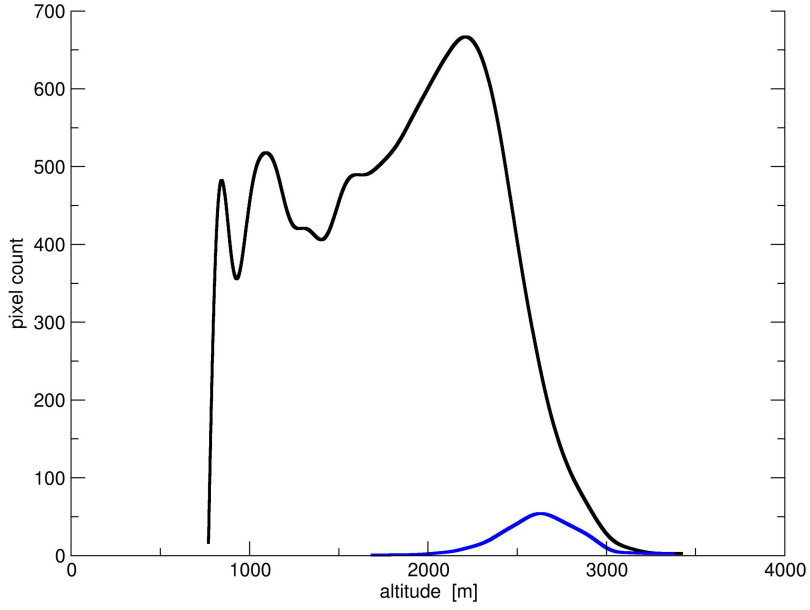

Figure 5. Hypsograph of the study area (glaciers marked with blue).

[31] Recall that this estimated glacier change will not be seen by the hydrologic modeling. It should be noted that the present glacier conditions are likely to be out of equilibrium already because of rising historic temperatures [*Stahl et al.*, 2008], so that studying the equilibrium response of glaciers is inaccurate. The extent to which this simplification affects the final result shall be discussed in section 5.

4. Results

[32] We start by displaying observed and simulated meteorological climates in Figure 7 on the basis of spatial averages of the site variables T and P. Here and in the following, when comparing present and future climatologies, we use the 20 year periods 1980 to 1999 and 2040 to 2059, respectively. We start with the present climate. For T, the annual cycle is well reproduced by both downscaled NCEP- and 20C3M-driven runs (errors of about ± 1°C). The overall spread is considerably larger for P; especially February and October show variations of almost 1 mm d^{-1}. For the future (A2), which we interpret relative to the simulated present (20C3M), a general increase of T of about 2°C is projected by most of the models. For P, no clear signal emerges from the future simulations (low signal-to-noise ratio). In general, more models predict decreasing monthly P (30 versus 18), especially from January to August, and

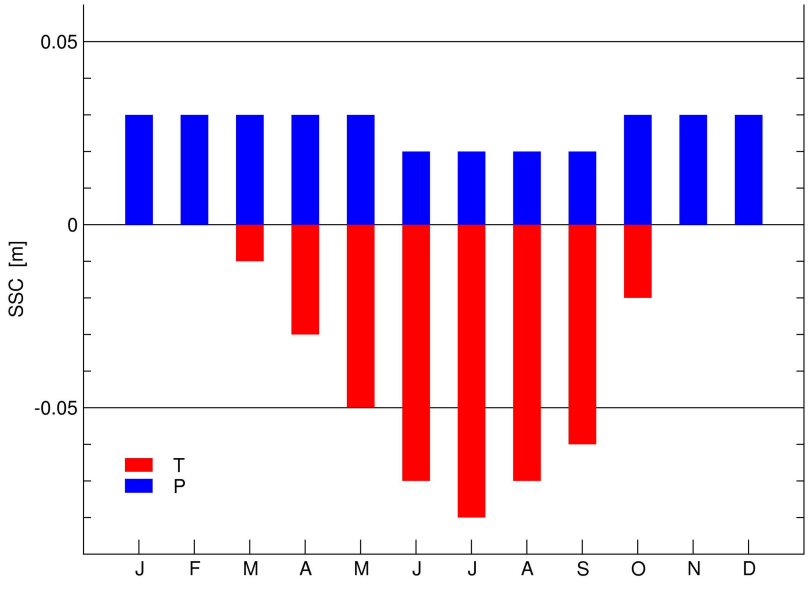

Figure 6. Seasonal sensitivity characteristics for the Peyto glacier [data from *Oerlemans and Reichert*, 2000]. Units are meters of water equivalent (per K for T and per 10% for P).

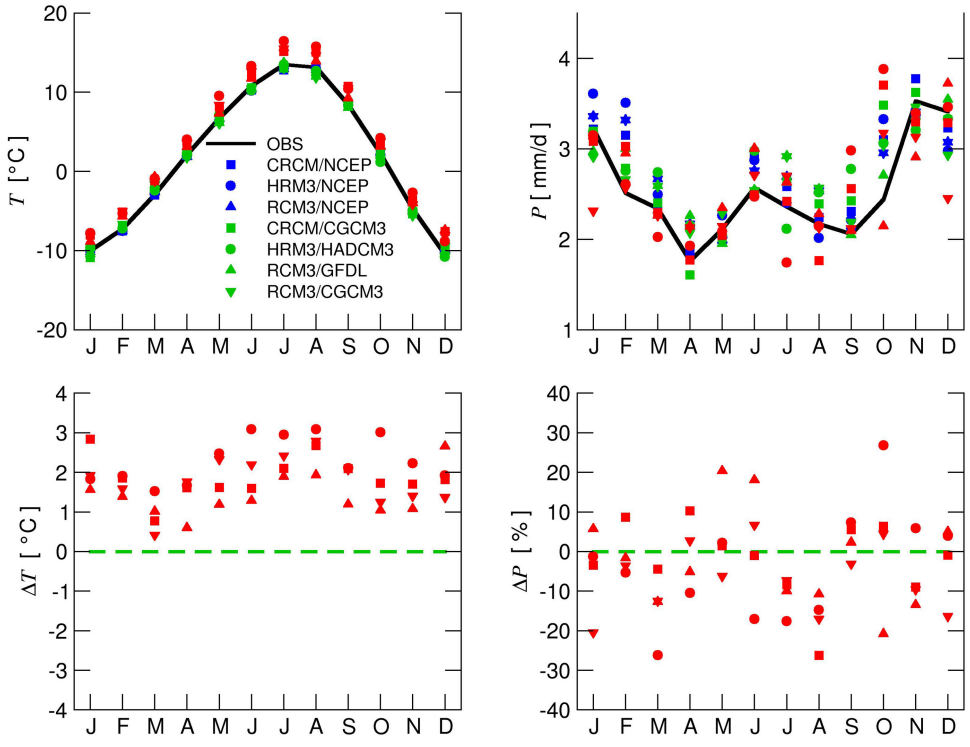

Figure 7. Observed (black line) and (left) downscaled average temperature T and (right) precipitation P, (top) in absolute values and (bottom) relative to the 20C3M simulations. Downscaling drivers are analyses (blue) and simulations from 20C3M (green) and A2 (red) emissions, using CRCM/CGCM3 (squares), HRM3/HADCM3 (circles), RCM3/GFDL (upward triangles), and RCM3/CGCM3 (downward triangles).

for the months of March, July, and August all models agree in predicting decreasing P. As there is noticeable uncertainty in the downscaled present P climate, it is conclusive to check whether bias correction and downscaling are actually capable of reducing any uncertainty that comes from the driving RCM fields. Figure 8 displays the spread of present monthly T and P climatologies from the downscaling and from raw RCM grids versus station observations. For temperature, there is an obvious cold bias in the RCM grid values, which simply reflects the undersampling of areal temperature by the stations (more exactly, the warm bias of the station average); the intermodel spread of almost 10°C is drastically reduced to one of ±1°C (see above). No systematic biases are seen for P, but there are very large discrepancies between the RCM results. Between HRM3 and CRCM, there are differences of more than 3 mm d^{-1}, which is about the absolute observed value. Hence, bias correction and downscaling appear to improve the simulated mean climate from the RCMs. The fact that not all of the spread is removed in the downscaled climates can be attributed to several factors: First, the displayed values are not based on the calibration period, so all estimates are suboptimal for this particular sample. Second, and most importantly, the probit normalization reflects the entire non-Gaussian daily distribution, including extremes, so that monthly statistics can be different, especially for P.

[33] We have analyzed the altitudinal profile of the projected climate change for T and P for the raw RCM and the downscaled data. By starting with the latter, Figure 9a illustrates for the downscaled station data that in all four scenarios the projected warming decreases with altitude, with a rate of roughly −0.3°C per 1000 m. The uncertainty of these trends is still large, and only those from RCM3 are significantly negative (based on a 5% level), but they are in overall agreement with observed trends in other mountainous areas [*Diaz and Bradley*, 1997; *Vuille and Bradley*, 2000]. They also correspond to a reported general reduction of warming in the free atmosphere [*Pepin and Seidel*, 2005]. For P, only the CRCM scenario shows a strong and significant decreasing tendency with height, which even includes a sign change at an altitude of about 1500 m. It is unknown whether this is in some way related to the better performance of CRCM (see Table 3). The large variations between the different stations are indicative of poor sampling, however. As Figure 9b illustrates, no corresponding attenuation of warming with height exists for the corresponding direct RCM scenarios when confined to the grid points that cover the study area. For P, no conclusive signal exists either; RCM3 even displays (significant) opposite trends when driven by GFDL (positive) and CGCM3 (negative). Note that the corresponding altitudinal range is much smaller in this case (1500–2200 m as compared to 800–2200 m for the stations). With regard to GCMs the climate signal is uniform as the study area is fully contained within one grid cell (of about 1300 m altitude). Altitudinal profiles of the RCM climate signal have been reported before, with partly opposite trends. For example, *Giorgi et al.* [1997] describe increased warming with altitude and attribute it to the positive snow-albedo feedback; similar trends are seen with precipitation. Their RCM results (using an older version of

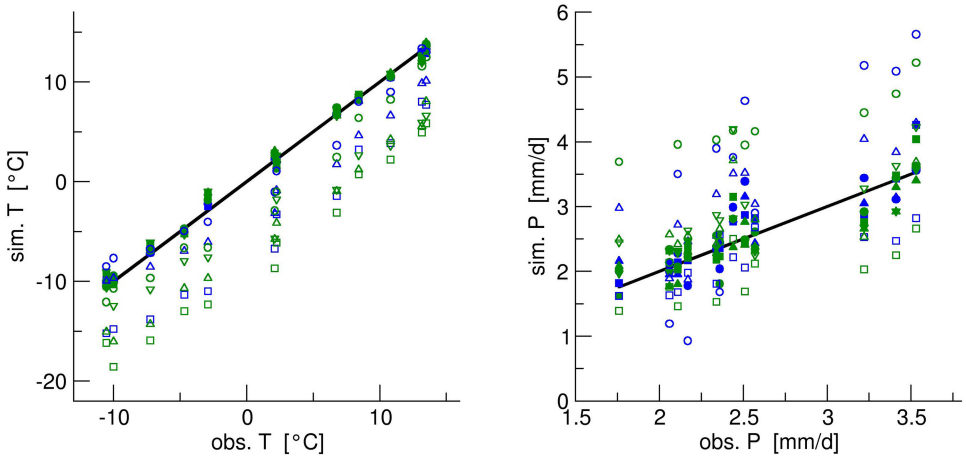

Figure 8. Scatter of simulated versus observed T and P monthly mean values for the present. Solid symbols are as in Figure 7, and open symbols are from regional climate models (RCMs), with the shapes corresponding to the solid symbols.

RCM3) are distinguished from ours by several aspects; most importantly, they apply to the entire elevational range below 2000 m; moreover, they are obtained for a larger and different area (Alps), so regional signals may confound the altitudinal signal.

[34] The altitudinal gradients (i.e., large range for relatively small area) typical of Figure 9a cannot be resolved by current gridded simulations (of ∼50 km grid length). One may wonder, therefore, how the increased detail in the statistical downscaling is obtained from the relatively uniform forcing. The only possible reason is the enhanced spatial detail in the statistical model itself, that is, in the matrix entries of EDS as shown in equation (1). From that, the downscaled future signal is a linear response of the main principal components of the large-scale predictor fields, and its altitudinal profile can be decomposed, approximately linearly, into profiles from the single components. As it turns out, for T_n and T_x the strongest altitudinal gradient is introduced by the dominant temperature component, for all scenarios. This is most likely due to a greater

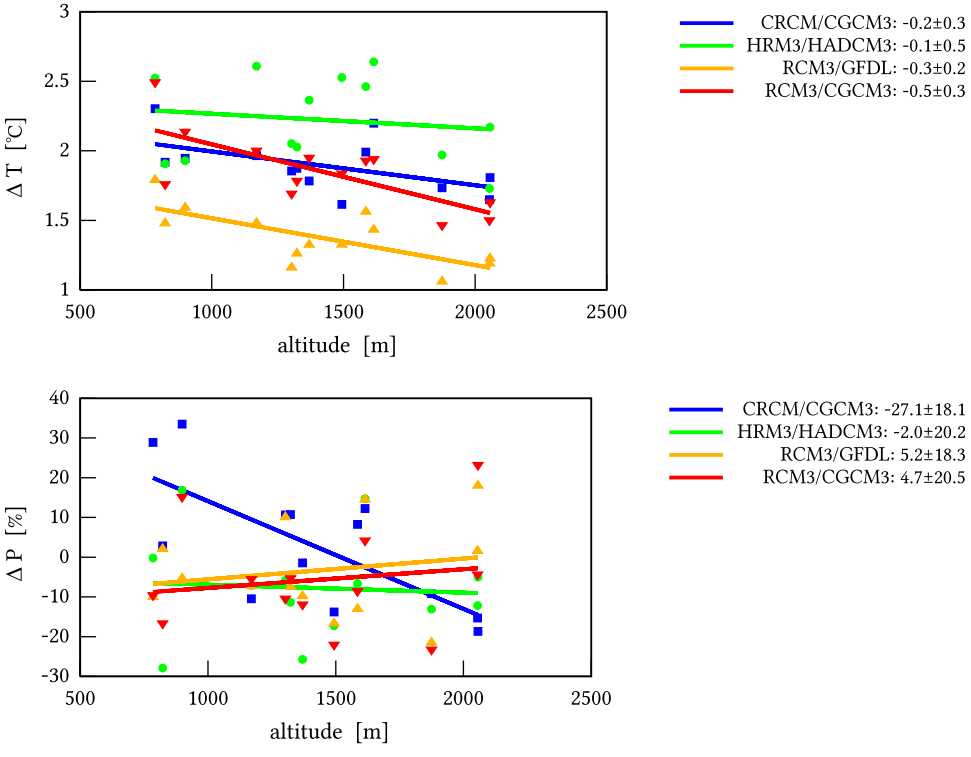

Figure 9a. Projected climate change of (top) T (in °C) and (bottom) P (in %) with station altitude. Symbols are as in Figure 7, and legend numbers are per 1000 m altitude change, with 95% confidence interval added.

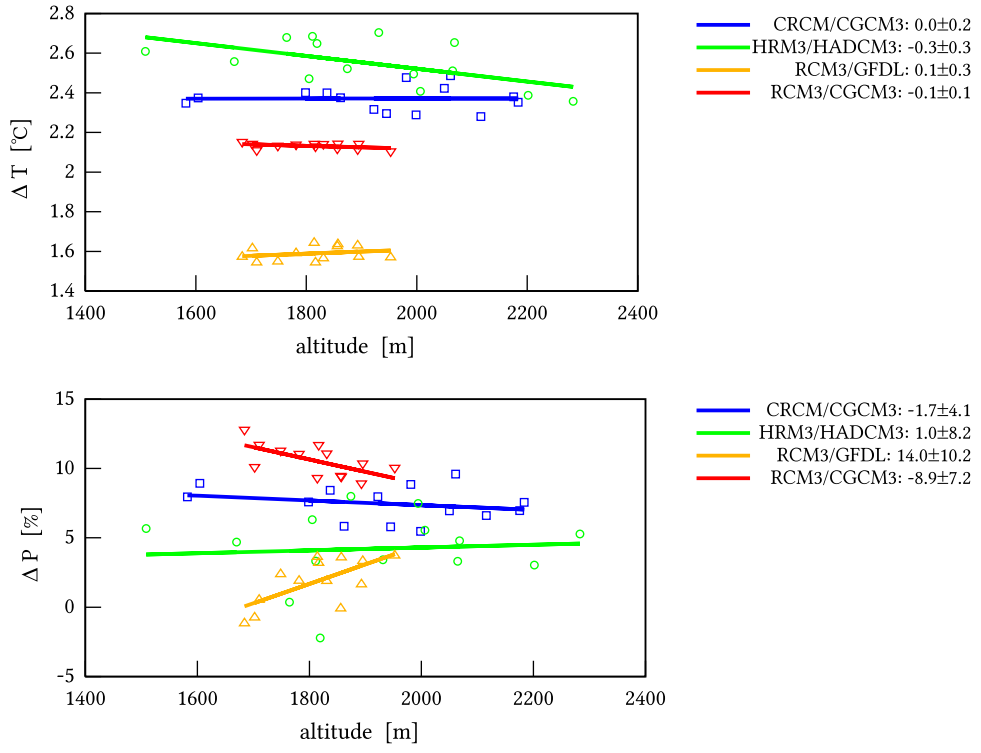

Figure 9b. As in Figure 9a, but for the direct RCM simulations based on the grid points covering the study area. Note that axis scales differ from those in Figure 9a.

sensitivity (i.e., correlation) to the large-scale signal at lower elevations. For *P*, the situation is complicated by the fact that besides the main temperature component, which creates a positive altitudinal trend in all scenarios, a similar trend of opposite sign is induced by the main humidity component, canceling the overall trend. As the balance between temperature and humidity components seems to be rather delicate and depends on the scenario, no conclusive picture emerges for *P* in general.

[35] Observed and NCEP-simulated streamflow at Donald between 1980 and 2002 are shown in Figure 10. Although in most years the main flow is matched by the simulations, there are notable exceptions for various models, such as underpredictions of the main peak in 1991 by all models or in 1986 by HRM3 and RCM3, or overprediction by RCM3 in 1988, 1996, and 1999. In comparison to errors due to imperfect WaSim parameterization and calibration and poor station coverage, the errors introduced by the downscaling are likely to be much larger. These are, most notably, residual reanalysis biases that cannot be corrected in a simple way and systematic limitations from the downscaling model (e.g., being linear). This is reflected in the resulting NSE values, shown in Table 3. The NSE drops from about 94% to about 80% for the four models for the calibration and the validation periods. Most errors result from misrepresented peak flow.

[36] Explaining about 80% of daily streamflow variations (up to 88% for the CRCM), the NCEP-driven simulations show satisfactory performance. Although most of this skill certainly comes from reproducing the annual cycle and thus provides fairly robust scenarios for the future hydrograph of the Columbia at Donald, it should give sufficient confidence in the corresponding estimates of future variability, including extremes. Figure 11 shows observed and simulated hydrographs for the various forcings. First of all, the hydrologic simulation for the present from meteorological observations is fairly accurate, with a slight overprediction during the early spring and summer months, especially for July. A larger error, as was to be expected, is introduced by using downscaled meteorology. The downscaled values tend to follow the hydrograph simulated from meteorological observations, which is expected because that is what they have been trained to; downscaled July to September flow is overestimated, however. Despite this imperfection, a relatively clear signal emerges from the future simulations if taken relative to the simulated present (20C3M), as above: For the first half year, all models project increasing flow, ranging up to about +60% for some. This is followed by a decrease of flow, as projected across all models, peaking in August by an average of 30%, and again increasing flow from October until the end of the year.

[37] To demonstrate the isolated effect of glacier melt, Figure 12 displays present and future hydrographs from the glaciated and nonglaciated basins separately. First, all projected hydrographs, whether or not glaciated basins are included, expose a shift from a snow- to a rain-dominated regime, with peak flow occurring in June instead of July. Apart from this, projections of the overall water balance are ambiguous, with CRCM/CGCM3 showing increasing levels and HRM3/HADCM3 showing decreasing levels. For the present, the runoff from glacier melt is only marginal, even in the summer months. For the future, at least two models (HRM3/HADCM3 and RCM3/CGCM3) project that this will change significantly, with the portion

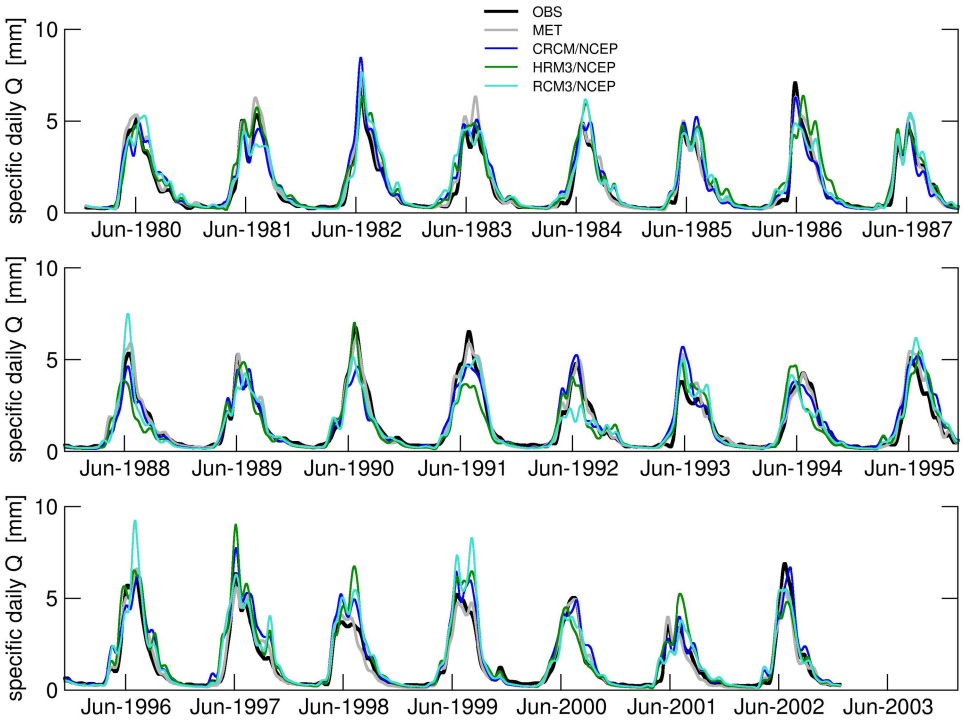

Figure 10. Streamflow (smoothed) from 1980 to 2003, as observed (gray line) and simulated from observations (black line) or downscaled NCEP analyses, using CRCM (blue line), HRM3 (green line), and RCM3 (turquoise line).

from glacier melt increasing to almost 50% in late summer. Here we probably see the cumulative effects of three different processes: first, the decreasing influence from snowmelt due to a smaller snowpack (shift of hydrograph); second, the reduced amount from direct rainfall, as displayed in Figure 7; and third, the increasing melt from glaciers, whose area has not diminished in the current static model setting.

[38] A rough estimate of future glacier extent and melt is obtained via equation (5) as follows: one gets the volume (as water equivalent) for each glacier in the study area. A glacier mass signal in response to the T and P signals (as areal average from the 2050s) is obtained from the SSC, equation (4), which can be translated back to an areal extent. The resulting average glacier change is listed in Table 4, revealing a general recession by 2050 of mass (area), ranging from 0.7 m (5.6%) to 1.3 m (9.5%) depending on the RCM, which roughly corresponds to the observed trends of the past 50 years [*Debeer and Sharp*, 2007] and is somewhat optimistic as compared to corresponding values of *Radic and Hock* [2011].

[39] For the 2050s the hydrologic model, whose static glacier hydrology does not see this retreat of glaciers, still simulates runoff from these then ice-free areas, which creates a considerable error. The error is particularly large for the late summer months, particularly errors in flow variability, which includes estimates of low and high flow. To still assess these extreme flow characteristics from our scenarios, we consider runoff generated solely from the nonglaciated basins. All extreme flow calculations are based on 3 day moving averages. In Figure 13 we see the simulated low flow for the month of August when the flow would have been primarily from glacier melt. Note that mean and variance for the present are in good agreement for all models. Except perhaps for HRM3, even the simulation of individual years is well captured. All simulations show a significant decline, with values varying around 1.2 mm d^{-1} for the present and 0.5 mm d^{-1} for the future, and then even zero flow is approached occasionally. High flow is shown in Figure 14. Again, the distribution of present values is represented fairly well, with the exception of RCM3, which shows overly extreme variations; individual years are less reliably reproduced. Only CRCM/CGCM3 remains fairly stationary in the future, while the other models show moderately decreasing high flow, with reductions of about 1 mm d^{-1}. The low-flow results are at odds with the report by *Hamlet et al.* [2010], which suggests rising levels for this area using an ensemble of 19 downscaled monthly GCM scenarios. This discrepancy can have many reasons, such as the use of different GCMs or different downscaling methods; additionally, the use of monthly scenarios as

Table 3. Nash-Sutcliffe Efficiency Performance Statistic (in %) for Streamflow at Donald, as Simulated by WaSim From Meteorological Observations and From Expanded Downscaling, RCM-Regionalized NCEP Fields for Calibration and Validation Periods

	Calibration (1990–1997)	Validation (1998–2002)
MET	94	95
CRCM3/NCEP	82	88
HRM3/NCEP	77	76
RCM3/NCEP	81	73

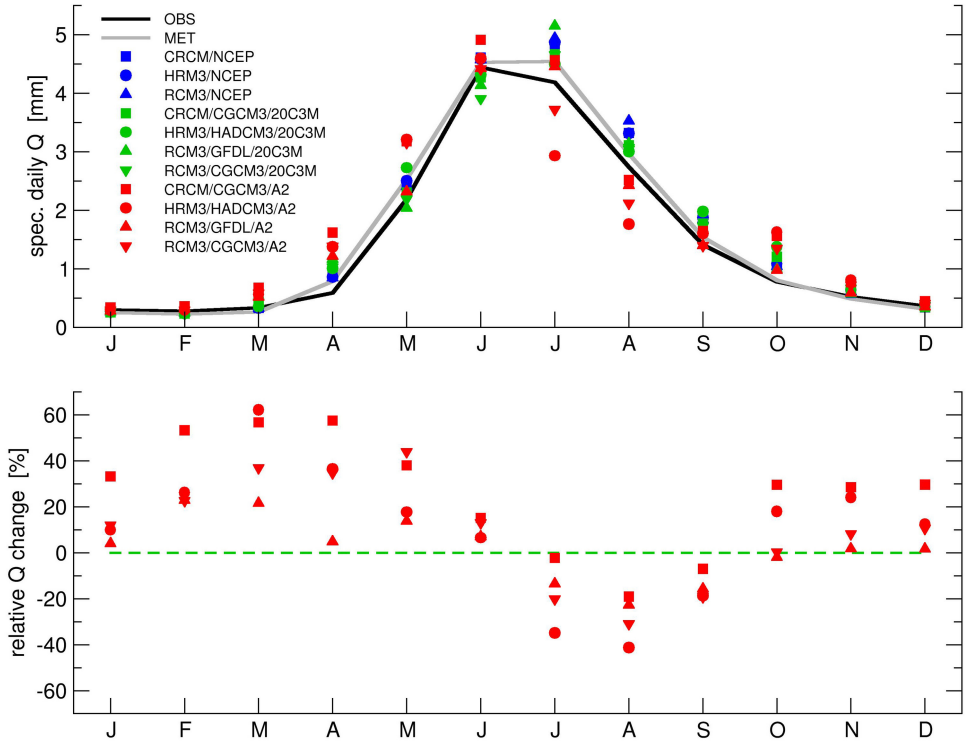

Figure 11. Observed (black line) and simulated annual hydrograph for Donald. Simulations are from observations (gray line) or from downscaling using the input of Figure 7 (with an identical color scheme). We show (top) absolute and (bottom) relative (to 20C3M) changes.

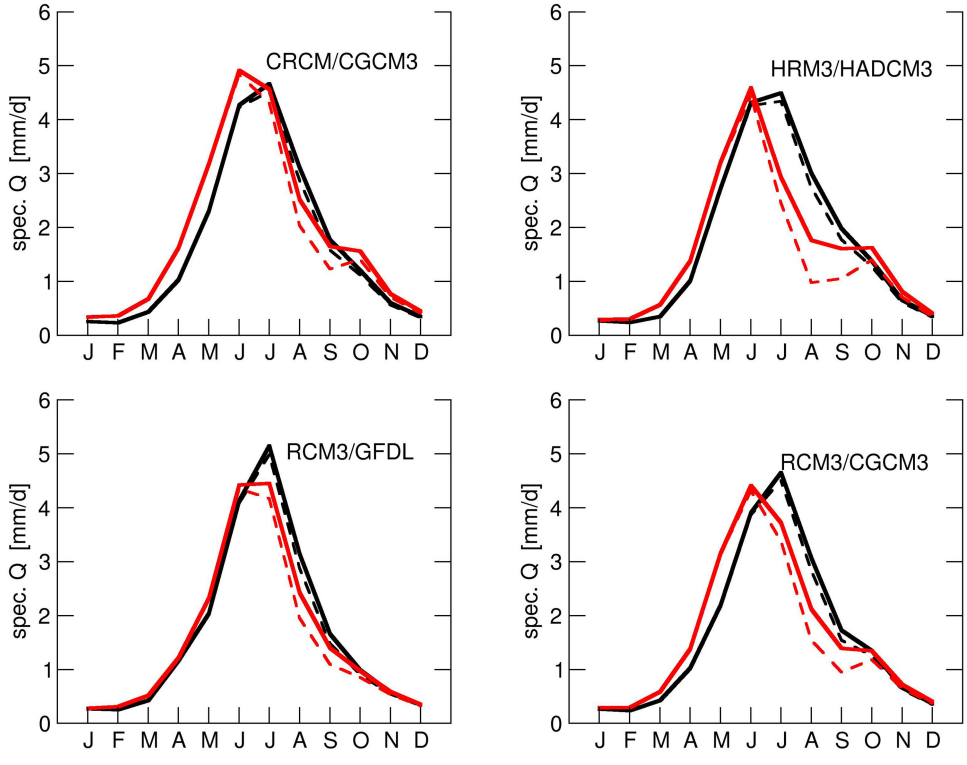

Figure 12. Specific discharge of full basin (solid lines) and of nonglaciated subbasins only (dashed lines) for the present (from 20C3M, black lines) and future (from A2, red lines) climates as simulated by the four different models.

Table 4. Average Change of Glacier Mass and Area Change

	CRCM/ CGCM3	HRM3/ HADCM3	RCM3/ GFDL	RCM3/ CGCM3
Mass (m water equivalent)	−0.78	−1.29	−0.74	−1.13
Area (%)	−5.9	−9.5	−5.6	−8.3

opposed to daily scenarios will likely influence the low-flow results as well.

5. Discussion

[40] We have provided projections of the future hydrograph, along with estimates of low and high flows of the Columbia River headwaters above Donald. The streamflow simulations form the end point of a cascade of four different model types: global and regional climate models (taken from the NARCCAP suite), a statistical downscaling model, and a hydrologic model. We have thoroughly verified this model chain for our purpose. Specifically, simulated streamflow from dynamically and statistically downscaled NCEP reanalyses could reproduce about 80% (88% for CRCM) of the actual daily streamflow variations at Donald. After bias correction, which was substantial for some models, using this model chain could simulate the present climate with enough confidence to derive future estimates of streamflow. In accordance with previous studies for similar areas all models projected a shift of the seasonal hydrograph by 1 month, with maximum flow now occurring in June instead of July. This is caused by winter precipitation falling increasingly as rain and snowpack melting earlier. Besides the shifting of the hydrograph the models somewhat disagree about possible changes in the overall flow; for example, CRCM/CGCM3 projects increasing annual flow, and HRM3/HADCM3 projects decreasing annual flow.

[41] Except for the late summer months, glacier melt contributes only marginally to the mean flow, and this is not likely to change in the future. Hence, the shift of the hydrologic regime is fairly independent of glacier dynamics, which we had to assume as constant in our hydrologic modeling. For peak flow, where glacier melt is likewise negligible, we have seen little change in the best performing model (CRCM) and decreasing values otherwise; accordingly, our results do not suggest increased flood risk for the area in the future. With respect to late summer low flow, however, the glacier response to a warming atmosphere is crucial. Our estimate showed a moderate glacier recession of about 10% for the 2050s, in accordance with observed recent trends; this is probably due to the moderate climate sensitivity of the Peyto glacier that was used. Hence, glaciers will almost certainly still contribute to late summer flow and may in the meantime even increasingly do so because of intensified melting from the higher temperatures. But even if they completely disappear, a full drought remains unlikely because of residual flow from the nonglaciated basins. But this flow displays an equally negative tendency from the decreasing late summer precipitation and occasionally even approaches zero, such as in the HRM3/HADCM3 simulation. In summary, while glacier melt may intermediately mitigate the negative tendency of late summer low flow, the long run poses a clear risk of drought, with obvious consequences for river habitat and agricultural and municipal shortages.

[42] The altitudinal profile of the climate signal, at least for temperature, i.e., the decreased warming with altitude from Figure 9a, appears to be a "real" feature of the scenarios, which is evidently important for the simulation of the snowline and all its hydrologic effects. As mentioned in section 3, the corresponding station-specific response is simply a consequence of the varying local correlations with the larger scales; as such, it is not unique to EDS and can be obtained by any skillful transfer function method. We only touched on this briefly in our study, but it is probably worth an extra study solely devoted to it, including a thorough verification based on a much denser station network than the one from this study, such as the Alps, and including an investigation into its potential physical causes. A subsequent sensitivity assessment of its hydrologic consequences is also important.

[43] Several of the above steps and results require attention. The simulated present climate from the GCMs revealed strong biases and required considerable correction, which introduces uncertainties into the present approach that are essentially unknown. Bias correction methods are known to evade verification as sufficient independent long-term climate variations are not available; however, as corrections they are at least valid to first order. Given the strong topographic gradients, a crucial element of the projection step is the climate sampling of the study area. Using merely 13 stations to estimate an area of almost 10,000 km^2 is certainly questionable, but it contains everything there is of original data, and the hydrologic model has employed a sophisticated interpolation technique to utilize topographic information (all gridded data sets for this area rely on this same sparse material). Our assessment of extremes required a downscaling approach that not only is based on daily statistics but also allows for these statistics to change, that is, one using daily GCM scenarios. Likewise, compared to gridded approaches that are more common and suitable for larger study areas, such as the entire Columbia basin, our downscaling approach applies directly to the original station data from the mountainous and glaciated Columbia headwaters, which gives it the flexibility of allowing an individual response from each station to the large-scale climate forcing (which it seems to have, in fact; see Figure 9a). This also includes, as we have seen, a greater sensitivity to the driving atmosphere, with potentially diverging future results, such as for peak flow, which was stationary only for CRCM. Given this diversity, one may be tempted to find the future simulations of CRCM more credible on the basis of the performance for the present from NCEP. But that means neglecting the important role of the GCM for future simulations, which may thus still be uncertain, even if driving other, possibly "superior" RCMs from the larger NARCCAP suite. For a full assessment, therefore, one has to wait until all possible GCM-RCM combinations of NARCCAP become available and then analyze their performance and future projections for the Columbia headwaters.

[44] One should also seek to combine the currently best possible gridded data sets, perhaps that of *Maurer et al.* [2002], with a point-based statistical downscaling that allows for a high-resolution climate response. Especially

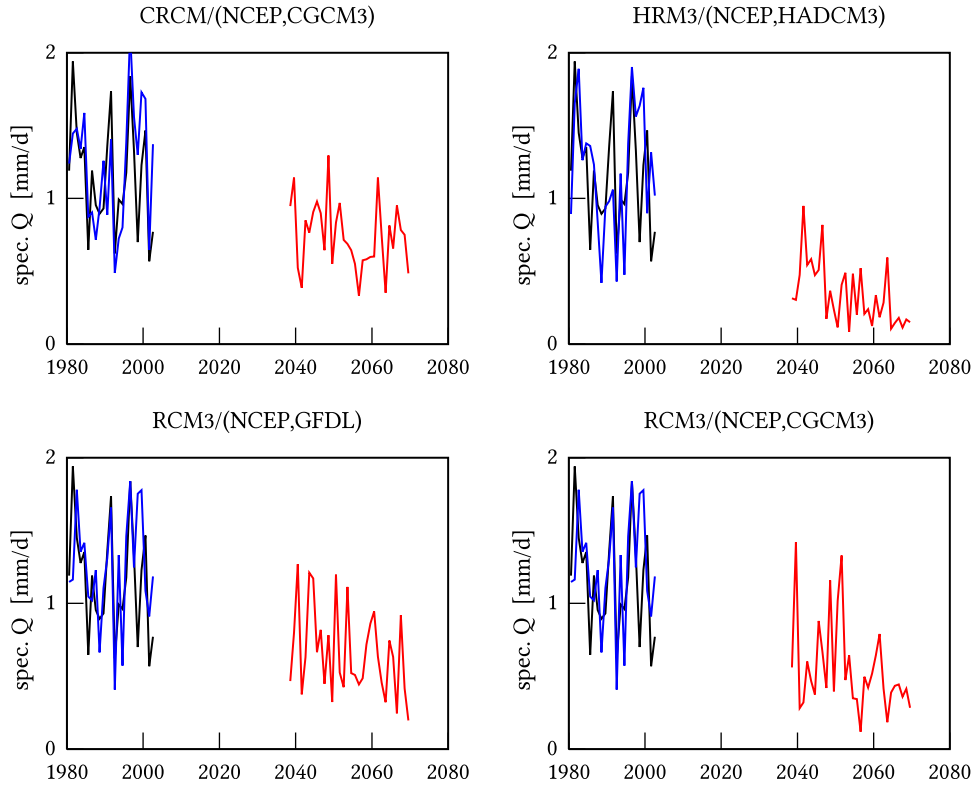

Figure 13. August low flow from nonglaciated subbasins, as simulated from observations (black line), NCEP (blue line), and climate scenarios (red line), using the four RCM/GCM combinations.

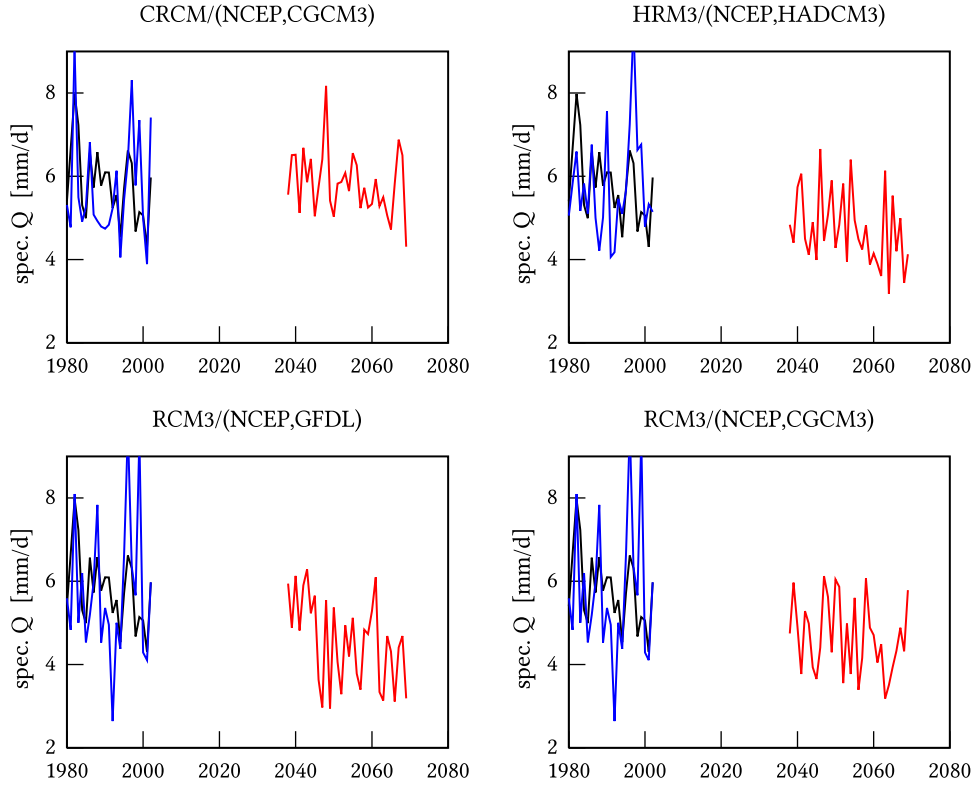

Figure 14. As in Figure 13, but for annual peak flow.

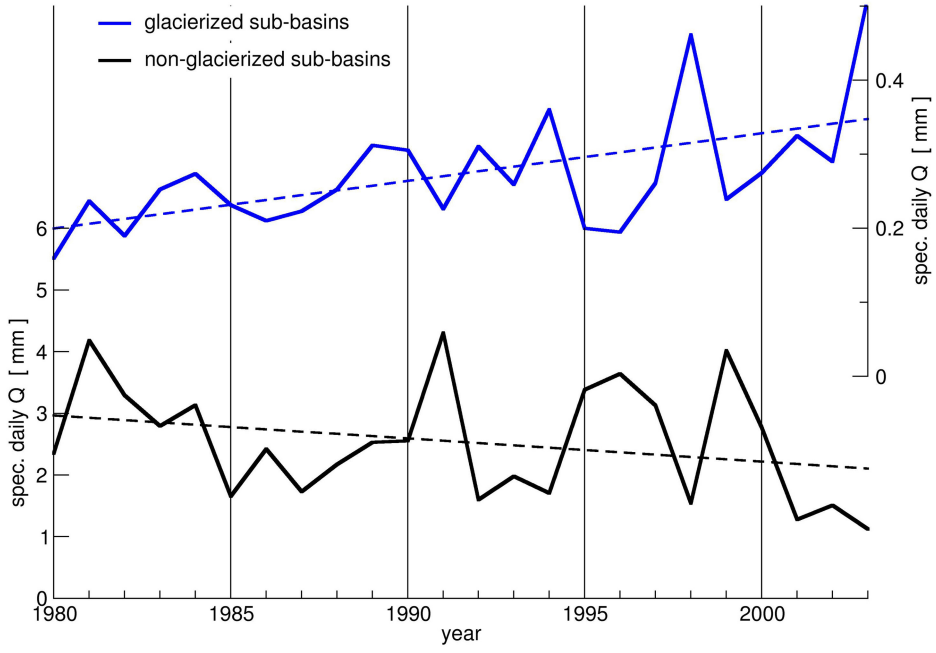

Figure 15. Simulated historic August streamflow from glaciated subbasins (blue line) and nonglaciated subbasins (black line). The glacier-induced streamflow has a significant positive trend.

the low-flow statistics have shown the importance of glacier dynamics. Our approach did not include any dynamics, but its heuristic assessment revealed that glacier response can be expected to be moderate for the 2050s, so that a static approach is a reasonable approximation a posteriori. A refined assessment that provides a more reliable evolution of drought risk through the present century would require dynamic glaciers, however. For example, if there is still enough glacier mass, enhanced melting under warmer conditions can compensate for the decrease in snowpack-induced flow from the shifted hydrograph, a decrease that is commonly observed in many basins of the Pacific Northwest [*Hamlet et al.*, 2005]. This compensating effect may also shed some light onto our introductory Figure 2, where the observed Columbia flow at Donald showed no significant trend. Our simulations from present meteorological observations reveal that, in fact, there is a significant positive trend in the glacier-induced portion of the river; see Figure 15. But again, this is based on static glaciers, and with real (dynamic) glaciers this has already weakened or will finally weaken and eventually end, so that summer streamflow becomes critically low. Exactly when this is to be expected can only be answered by a fully dynamic hydrologic glacier component. A version of WaSim that supports dynamic glaciers is currently under development.

Appendix A: Multivariate Bias Correction

[45] Any simulation of present climate, say for a variable $\mathbf{x}$, is given as

$$\tilde{\mathbf{x}} = \hat{\mathbf{x}} + \boldsymbol{\varepsilon}_m + \boldsymbol{\varepsilon}_s - \boldsymbol{\varepsilon}_o, \tag{A1}$$

where $\hat{\mathbf{x}}$ indicates observations, the subscript m refers to model bias, and o and s refer to bias from observations and simulations, respectively. The only quantities that are actually known are $\hat{\mathbf{x}}$ and $\tilde{\mathbf{x}}$, and accordingly, the overall bias $\boldsymbol{\varepsilon}_m + \boldsymbol{\varepsilon}_s - \boldsymbol{\varepsilon}_o = \langle\tilde{\mathbf{x}}\rangle - \langle\hat{\mathbf{x}}\rangle$. Unless the simulation has very different memory than the observations, $\boldsymbol{\varepsilon}_o$ and $\boldsymbol{\varepsilon}_s$ are equally distributed and should be of the same scale. By assuming now that this scale is small relative to $\boldsymbol{\varepsilon}_m$, the overall bias $\boldsymbol{\varepsilon}_m + \boldsymbol{\varepsilon}_s + \boldsymbol{\varepsilon}_o$ can be estimated with $\boldsymbol{\varepsilon}_m$. Subtracting this overall bias,

$$\tilde{\mathbf{x}} \quad \mapsto \quad \tilde{\mathbf{x}} - (\langle\tilde{\mathbf{x}}\rangle - \langle\hat{\mathbf{x}}\rangle), \tag{A2}$$

amounts to the removal of the model bias $\boldsymbol{\varepsilon}_m$ from the simulations and is usually referred to as bias correction of the mean.

[46] After having corrected for the mean, the remaining (anomaly) series, $\tilde{\delta}\mathbf{x}$ and $\bar{\delta}\mathbf{x}$, can be further adjusted to account for variance biases. Essentially, by replacing addition with multiplication in equation (A2), the variance bias adjustment would be $\tilde{\delta}\mathbf{x}\tilde{\delta}\mathbf{x}\sigma_{\bar{\mathbf{x}}}/\sigma_{\tilde{\mathbf{x}}}$. In the multivariate case, the standard deviation (square root of the variance) has to be replaced by the Cholesky factor of the covariance matrix. Specifically, if $\mathbf{C}_{\hat{\mathbf{x}}} \mapsto \mathbf{G}_{\hat{\mathbf{x}}}\mathbf{G}_{\hat{\mathbf{x}}}^{'}$ and $\mathbf{C}_{\tilde{\mathbf{x}}} \mapsto \mathbf{G}_{\tilde{\mathbf{x}}}\mathbf{G}_{\tilde{\mathbf{x}}}^{'}$ are the Cholesky decompositions of the covariance matrices of $\hat{\mathbf{x}}$ and $\tilde{\mathbf{x}}$, respectively, then multivariate bias correction is done as follows:

$$\tilde{\delta}\mathbf{x}\tilde{\delta}\mathbf{x}\ \mathbf{G}_{\tilde{\mathbf{x}}}^{-1}\ \mathbf{G}_{\bar{\mathbf{x}}}. \tag{A3}$$

[47] Anomalies have been calculated relative to the climate under consideration (e.g., the 2050s). One could also use the present climate, but then one must be aware that any climate change signal gets "corrected" as well. Note that for this form of bias correction the quantities should be Gaussian because otherwise their variability is only imperfectly reflected by the covariance.

[48] **Acknowledgments.** We enjoyed fruitful discussions with Markus Schnorbus. Hailey Eckstrand and Anne Berland helped to prepare the figures. This study was made possible through generous funding from the BC Ministry of Environment and BC-Hydro.

References

Alpert, P. (1986), Mesoscale indexing of the distribution of orographic precipitation over high mountains, *J. Clim. Appl. Meteorol.*, *25*(4), 532–545.

Bahr, D. B., M. F. Meier, and S. D. Peckham (1997), The physical basis of glacier volume-area scaling, *J. Geophys. Res.*, *102*, 20,355–20,362, doi:10.1029/97JB01696.

Barnett, T. P., J. C. Adam, and D. P. Lettenmaier (2005), Potential impacts of a warming climate on water availability in snow-dominated regions, *Nature*, *438*(7066), 303–309.

Barnett, T. P., et al. (2008), Human-induced changes in the hydrology of the western United States, *Science*, *319*(5866), 1080–1083.

Barros, A. P., and D. P. Lettenmaier (1994), Dynamic modeling of orographically induced precipitation, *Rev. Geophys.*, *32*(3), 265–284, doi:10.1029/94RG00625.

Bitz, C. M., and D. S. Battisti (1999), Interannual to decadal variability in climate and the glacier mass balance in Washington, Western Canada, and Alaska, *J. Clim.*, *12*(11), 3181–3196.

Bolch, T., B. Menounos, and R. Wheate (2010), Landsat-based inventory of glaciers in western Canada, 1985–2005, *Remote Sens. Environ.*, *114*(1), 127–137.

Braithwaite, R. J., Y. Zhang, and S. C. B. Raper (2002), Temperature sensitivity of the mass balance of mountain glaciers and ice caps as a climatological characteristic, *Z. Gletscherkd. Glazialgeol.*, *38*(1), 35–61.

Bürger, G. (1996), Expanded downscaling for generating local weather scenarios, *Clim. Res.*, *7*, 111–128.

Bürger, G. (2002), Selected precipitation scenarios across Europe, *J. Hydrol.*, *262*(1–4), 99–110.

Bürger, G. (2009), Dynamically vs. empirically downscaled medium-range precipitation forecasts, *Hydrol. Earth Syst. Sci.*, *13*(9), 1649–1658.

Bürger, G., and Y. Chen (2005), Regression-based downscaling of spatial variability for hydrologic applications, *J. Hydrol.*, *311*(1–4), 299–317.

Bürger, G., D. Reusser, and D. Kneis (2009), Early flood warnings from empirical (expanded) downscaling of the full ECMWF Ensemble Prediction System, *Water Resour. Res.*, *45*, W10443, doi:10.1029/2009WR007779.

Caya, D., and R. Laprise (1999), A semi-implicit semi-Lagrangian regional climate model: The Canadian RCM, *Mon. Weather Rev.*, *127*(3), 341–362.

Cayan, D. R. (1996), Interannual climate variability and snowpack in the western United States, *J. Clim.*, *9*(5), 928–948.

Chen, J., and A. Ohmura (1990), Estimation of Alpine glacier water resources and their change since the 1870s, in *Hydrology in Mountainous Regions: 1. Hydrologic Measurements, the Water Cycle*, IAHS Publ., *193*, 127–135.

Debeer, C. M., and M. J. Sharp (2007), Recent changes in glacier area and volume within the southern Canadian Cordillera, *Ann. Glaciol.*, *46*(1), 215–221.

Déry, S. J., K. Stahl, R. D. Moore, P. H. Whitfield, B. Menounos, and J. E. Burford (2009), Detection of runoff timing changes in pluvial, nival, and glacial rivers of western Canada, *Water Resour. Res.*, *45*, W04426, doi:10.1029/2008WR006975.

Diaz, H. F., and R. S. Bradley (1997), Temperature variations during the last century at high elevation sites, *Clim. Change*, *36*, 253–279.

Dryden, I. L., and K. V. Mardia (1998), *Statistical Shape Analysis*, John Wiley, Chichester, U. K.

Elsner, M. M., L. Cuo, N. Voisin, J. S. Deems, A. F. Hamlet, J. A. Vano, K. E. B. Mickelson, S. Y. Lee, and D. P. Lettenmaier (2009), Implications of 21st century climate change for the hydrology of Washington State, *Clim. Change*, *102*, 1–36.

Environment Canada (2007), Canadian Daily Climate Data, Meteorol. Serv., Downsview, Ontario, Canada, CD-ROM.

Flowers, G. E., S. J. Marshall, H. Björnsson, and G. K. C. Clarke (2005), Sensitivity of Vatnajökull ice cap hydrology and dynamics to climate warming over the next 2 centuries, *J. Geophys. Res.*, *110*, F02011, doi:10.1029/2004JF000200.

Giorgi, F., J. W. Hurrell, M. R. Marinucci, and M. Beniston (1997), Elevation dependency of the surface climate change signal: A model study, *J. Clim.*, *10*(2), 288–296.

Global Soil Data Task Group (2000), Global Soil Data Products CD-ROM (IGBP-DIS), http://daac.ornl.gov/SOILS/igbp.html, Oak Ridge Natl. Lab. Distrib. Active Arch. Cent., Oak Ridge, Tenn.

Hamlet, A. (2010), Assessing water resources adaptive capacity to climate change impacts in the Pacific Northwest Region of North America, *Hydrol. Earth Syst. Sci. Discuss.*, *7*, 4437–4471.

Hamlet, A. F., and D. P. Lettenmaier (1999), Effects of climate change on hydrology and water resources in the Columbia River basin, *J. Am. Water Resour. Assoc.*, *35*(6), 1597–1623.

Hamlet, A. F., P. W. Mote, M. P. Clark, and D. P. Lettenmaier (2005), Effects of temperature and precipitation variability on snowpack trends in the western United States, *J. Clim.*, *18*(21), 4545–4561.

Hamlet, A. F., et al. (2010), Final project report for the Columbia Basin Climate Change Scenarios Project, Clim. Impacts Group, Univ. of Wash., Seattle. [Available at http://www.hydro.washington.edu/2860/report.]

Hamon, W. R. (1963), Computation of direct runoff amounts from storm rainfall, *IASH Publ.*, *63*, 52–62.

Hawkins, E., and R. Sutton (2009), The potential to narrow uncertainty in regional climate predictions, *Bull. Am. Meteorol. Soc.*, *90*(8), 1095–1107.

Hudson, D. A., and R. G. Jones (2002), Regional climate model simulations of present-day and future climates of southern Africa, *Tech. Note 39*, Met Off. Hadley Cent., Exeter, U. K.

Huss, M., S. Sugiyama, A. Bauder, and M. Funk (2007), Retreat scenarios of Unteraargletscher, Switzerland, using a combined ice-flow mass-balance model, *Arct. Antarct. Alp. Res.*, *39*(3), 422–431.

Huss, M., D. Farinotti, A. Bauder, and M. Funk (2008), Modelling runoff from highly glacierized alpine drainage basins in a changing climate, *Hydrol. Processes*, *22*(19), 3888–3902.

Intergovernmental Panel on Climate Change (2000), *Special Report on Emissions Scenarios*, edited by N. Nakicenovic and R. Swart Cambridge Univ. Press, New York.

Kanamitsu, M., W. Ebisuzaki, J. Woollen, S. K. Yang, J. J. Hnilo, M. Fiorino, and G. L. Potter (2002), NCEP-DOE AMIP-II Reanalysis (R-2), *Bull. Am. Meteorol. Soc.*, *83*(11), 1631–1643.

Knowles, N., M. D. Dettinger, and D. R. Cayan (2006), Trends in snowfall versus rainfall in the western United States, *J. Clim.*, *19*(18), 4545–4559, doi:10.1175/JCLI3850.1.

Lemke, P., et al. (2007), Observations: Changes in snow, ice and frozen ground, in *Climate Change 2007: The Physical Science Basis. Contribution of Working Group I to the Fourth Assessment Report of the Intergovernmental Panel on Climate Change*, edited by D. Qin et al., pp. 337–383, Cambridge Univ. Press, New York.

Leung, L. R., A. F. Hamlet, D. P. Lettenmaier, and A. Kumar (1999), Simulations of the ENSO hydroclimate signals in the Pacific Northwest Columbia River basin, *Bull. Am. Meteorol. Soc.*, *80*(11), 2313–2329.

Loukas, A., L. Vasiliades, and N. R. Dalezios (2004), Climate change implications on flood response of a mountainous watershed, *Water Air Soil Pollut. Focus*, *4*(4), 331–347.

Luckman, B., and T. Kavanagh (2000), Impact of climate fluctuations on mountain environments in the Canadian Rockies, *Ambio*, *29*(7), 371–380.

Maurer, E., A. Wood, J. Adam, D. Lettenmaier, and B. Nijssen (2002), A long-term hydrologically based dataset of land surface fluxes and states for the conterminous United States, *J. Clim.*, *15*(22), 3237–3251.

Maurer, E. P., H. G. Hidalgo, T. Das, M. D. Dettinger, and D. R. Cayan (2010), The utility of daily large-scale climate data in the assessment of climate change impacts on daily streamflow in California, *Hydrol. Earth Syst. Sci.*, *14*(6), 1125–1138.

McCabe, G. J., and M. D. Dettinger (2002), Primary modes and predictability of year-to-year snowpack variations in the western United States from teleconnections with Pacific Ocean climate, *J. Hydrometeorol.*, *3*(1), 13–25.

McCabe, G. J., M. A. Palecki, and J. L. Betancourt (2004), Pacific and Atlantic Ocean influences on multidecadal drought frequency in the United States, *Proc. Natl. Acad. Sci. U. S. A.*, *101*(12), 4136–4141.

Mearns, L., et al. (2005), NARCCAP North American Regional Climate Change Assessment Program: A multiple AOGCM and RCM climate scenario project over North America, American Meteorological Society 16th Conference on Climate Variations and Change, Am. Meteorol. Soc., Washington, D. C., paper J6.10, preprints pp. 235–238.

Meehl, G. A., C. Covey, B. McAvaney, M. Latif, and R. J. Stouffer (2005), Overview of the coupled model intercomparison project, *Bull. Am. Meteorol. Soc.*, *86*(1), 89–93.

Meehl, G. A., et al. (2007), Global climate projections, in *Climate Change 2007: The Physical Science Basis. Contribution of Working Group I to the Fourth Assessment Report of the Intergovernmental Panel on Climate Change*, edited by D. Qin et al., pp. 747–845, Cambridge Univ. Press, New York.

Menzel, L., and G. Bürger (2002), Climate change scenarios and runoff response in the Mulde catchment (southern Elbe, Germany), *J. Hydrol.*, *267*(1–2), 53–64.

Menzel, L., A. H. Thieken, D. Schwandt, and G. Bürger (2006), Impact of climate change on the regional hydrology–Scenario-based modelling studies in the German Rhine catchment, *Nat. Hazards*, *38*(1), 45–61.

Mote, P. W., A. F. Hamlet, M. P. Clark, and D. P. Lettenmaier (2005), Declining mountain snowpack in western North America, *Bull. Am. Meteorol. Soc.*, *86*(1), 39–49.

Müller-Wohlfeil, D. I., G. Bürger, and W. Lahmer (2000), Response of a river catchment to climate change: Application of expanded downscaling to northern Germany, *Clim. Change*, *47*, 61–89.

Nolin, A. W., J. Phillippe, A. Jefferson, and S. L. Lewis (2010), Present-day and future contributions of glacier runoff to summertime flows in a Pacific Northwest watershed: Implications for water resources, *Water Resour. Res.*, *46*, W12509, doi:10.1029/2009WR008968.

Oerlemans, J., and B. K. Reichert (2000), Relating glacier mass balance to meteorological data by using a seasonal sensitivity characteristic, *J. Glaciol.*, *46*(152), 1–6.

Oerlemans, J., et al. (1998), Modelling the response of glaciers to climate warming, *Clim. Dyn.*, *14*(4), 267–274.

Pal, J. S., et al. (2006), The ICTP RegCM3 and RegCNET: Regional climate modeling for the developing world, *Bull. Am. Meteorol. Soc.*, *88*, 1395–1409.

Payne, J. T., A. W. Wood, A. F. Hamlet, R. N. Palmer, and D. P. Lettenmaier (2004), Mitigating the effects of climate change on the water resources of the Columbia River basin, *Clim. Change*, *62*, 233–256.

Pepin, N., and D. J. Seidel (2005), A global comparison of surface and free-air temperatures at high elevations, *J. Geophys. Res.*, *110*, D03104, doi:10.1029/2004JD005047.

Radic, V., and R. Hock (2011), Regionally differentiated contribution of mountain glaciers and ice caps to future sea-level rise, *Nat. Geosci*, *4*(2), 91–94, doi:10.1038/ngeo1052.

Salathe, E. P., Jr. (2005), Downscaling simulations of future global climate with application to hydrologic modelling, *Int. J. Climatol.*, *25*(4), 419–436.

Schaefli, B., B. Hingray, M. Niggli, and A. Musy (2005), A conceptual glacio-hydrological model for high mountainous catchments, *Hydrol. Earth Syst. Sci.*, *9*(1/2), 95–109.

Schiefer, E., B. Menounos, and R. Wheate (2007), Recent volume loss of British Columbian glaciers, Canada, *Geophys. Res. Lett.*, *34*, L16503, doi:10.1029/2007GL030780.

Schneeberger, C., H. Blatter, A. Abe-Ouchi, and M. Wild (2003), Modelling changes in the mass balance of glaciers of the Northern Hemisphere for a transient 2xCO2 scenario, *J. Hydrol.*, *282*(1–4), 145–163.

Schulla, J. (1997), *Hydrologische Modellierung von Flussgebieten zur Abschätzung der Folgen von Klimaänderungen*, Geogr. Inst., Eidg. Tech. Hochsch., Zurich, Switzerland.

Schulla, J., and K. Jasper (2000), Model description WaSiM-ETH, report, Inst. for Atmos. and Clim. Sci., Swiss Fed. Inst. of Technol., Zürich.

Schulla, J., and K. Jasper (2007), Model description WaSiM-ETH, technical report, ETH, Zürich, Switzerland. [Available at http://www.wasim.ch.]

Stahl, K., and R. D. Moore (2006), Influence of watershed glacier coverage on summer streamflow in British Columbia, Canada, *Water Resour. Res.*, *42*, W06201, doi:10.1029/2006WR005022.

Stahl, K., R. D. Moore, J. M. Shea, D. Hutchinson, and A. J. Cannon (2008), Coupled modelling of glacier and streamflow response to future climate scenarios, *Water Resour. Res.*, *44*, W02422, doi:10.1029/2007WR005956.

Stewart, I. T., D. R. Cayan, and M. D. Dettinger (2005), Changes toward earlier streamflow timing across western North America, *J. Clim.*, *18*(8), 1136–1155, doi:10.1175/JCLI3321.1.

Vano, J. A., M. J. Scott, N. Voisin, C. O. Stöckle, A. F. Hamlet, K. E. B. Mickelson, M. M. G. Elsner, and D. P. Lettenmaier (2010a), Climate change impacts on water management and irrigated agriculture in the Yakima River Basin, Washington, USA, *Clim. Change*, *102*, 287–317.

Vano, J. A., N. Voisin, L. Cuo, A. F. Hamlet, M. M. G. Elsner, R. N. Palmer, A. Polebitski, and D. P. Lettenmaier (2010b), Climate change impacts on water management in the Puget Sound region, Washington State, USA, *Clim. Change*, *102*, 261–286.

Vuille, M., and R. S. Bradley (2000), Mean annual temperature trends and their vertical structure in the tropical Andes, *Geophys. Res. Lett.*, *27*(23), 3885–3888, doi:10.1029/2000GL011871.

Wang, S. Y., R. R. Gillies, E. S. Takle, and W. J. Gutowski Jr. (2009), Evaluation of precipitation in the intermountain region as simulated by the NARCCAP regional climate models, *Geophys. Res. Lett.*, *36*, L11704, doi:10.1029/2009GL037930.

Wilby, R. L., and T. M. L. Wigley (1997), Downscaling general circulation model output: A review of methods and limitations, *Prog. Phys. Geogr.*, *21*(4), 530–548.

Wood, A., E. Maurer, A. Kumar, and D. P. Lettenmaier (2002), Long-range experimental hydrologic forecasting for the eastern United States, *J. Geophys. Res.*, *107*(D20), 4429, doi:10.1029/2001JD000659.

G. Bürger, J. Schulla, and A. T. Werner, Pacific Climate Impacts Consortium, University of Victoria, University House 1, PO Box 3060 Stn CSC, Victoria, BC V8W 3R4, Canada. (gbuerger@uvic.ca)